Reprinted from OPHTHALMOLOGY, Vol. 103, No. 11, November 1996
Published by Lippincott–Raven Publishers Printed in U.S.A.

Direct Objective Quantification of Corneal Haze after Excimer Laser Photorefractive Keratectomy for High Myopia

Miguel J. Maldonado, MD, Vicente Arnau, PhD, Amparo Navea, MD, PhD, Rafael Martínez-Costa, MD, PhD, Francisco M. Mico, MS, Angel L. Cisneros, MD, José L. Menezo, MD, PhD

Direct Objective Quantification of Corneal Haze after Excimer Laser Photorefractive Keratectomy for High Myopia

Miguel J. Maldonado, MD,[1] Vicente Arnau, PhD,[2] Amparo Navea, MD, PhD,[1] Rafael Martínez-Costa, MD, PhD,[1] Francisco M. Mico, MS,[3] Angel L. Cisneros, MD,[1] José L. Menezo, MD, PhD[1]

Purpose: The purpose of the study is to measure regional distribution differences in corneal haze after excimer laser photorefractive keratectomy for high myopia.

Methods: The authors developed computerized gradient edge detectors with which were analyzed digitized anterior slit-lamp photographs of 40 eyes, an average of 21.0 plus or minus 14.5 weeks after photorefractive keratectomy for high myopia (−6 to −22 diopters). A treated area and an adjacent untreated area on the anterior corneal surface, each containing six regions, were quantified, and the difference was correlated with various parameters.

Results: Mean differences between scarred and clear areas for haze grade 0.5, 1.0, 2.0, 3.0, and 4.0 were 16.9, 26.6, 42.6, 60.4, and 76.4 gray levels, respectively (r_s = 0.96; P = 0.0001). A low but statistically significant correlation between the intended correction and postoperative corneal haze was found (r = 0.33; P = 0.037). The mean coefficient of variation of the amount of opacification within each treated area was 9.4%. This coefficient of variation increased with a longer follow-up time (r = 0.88; P = 0.0001). The difference in the intensity of haze between the center and more peripheral regions over the entrance pupil did not correlate with the attempted correction. However, a strong association between a relatively less severe central corneal haze with respect to more peripheral haze and longer follow-up time was found (r = −0.96; P = 0.0001).

Conclusion: The amount of corneal haze showed a weak positive association with the attempted correction in excimer laser photorefractive keratectomy for high myopia. Corneal haze appeared fairly uniformly distributed within the ablation zone, but a more heterogeneous distribution was found with a longer follow-up time. Furthermore, later postoperative examinations disclosed a clear trend toward diminishing central opacification relative to peripheral regions over the entrance pupil.

Ophthalmology 1996;103:1970–1978

Originally received: November 17, 1995.
Revision accepted: June 18, 1996.

[1] Department of Ophthalmology, La Fe University Hospital; Department of Surgery, University of Valencia, Valencia, Spain.

[2] Institute of Robotics, University of Valencia, Valencia, Spain.

[3] Department of Electrical Engineering and Computer Science, University of Valencia, Valencia, Spain.

Presented as a poster at the American Academy of Ophthalmology Annual Meeting, Atlanta, Oct/Nov 1995.

Reprint requests to Miguel J. Maldonado, MD, Servicio de Oftalmología, Hospital Universitario La Fe, Av. Campanar, no. 21, 46009 Valencia, Spain.

Although loss of corneal transparency is an important factor influencing the outcome of excimer laser corneal surgery,[1] little is known about its development and postoperative course. Previous experience shows that corrections of high myopia (more than 6 diopters) are associated with greater corneal opacity than are corrections of low and moderate myopia.[1] Corneal haze also has been reported to increase progressively to a maximum between 3 and 6 months after surgery and then to regress slowly.[2–4] Late corneal haze with the discontinuation of steroid therapy, however, has been observed more than

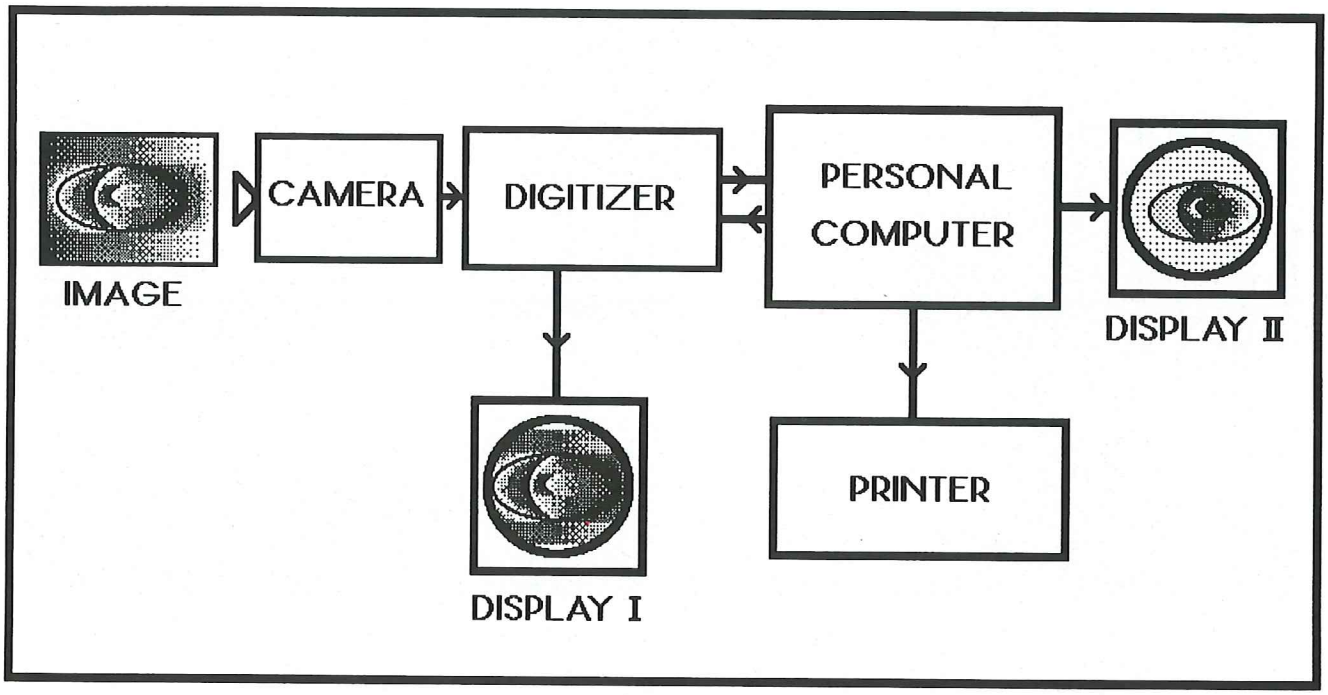

Figure 1. Schematic diagram of the system. The image acquisition module has a television signal as the input and converts this signal into digital form, both spatially and in amplitude. The video digitizer consists of a set of hardware modules that perform four basic functions: (1) image acquisition, (2) storage, (3) fast processing, and (4) display. The original image can be seen on the television monitor (display I), whereas the processed gradient image can be observed on the monitor of the personal computer (display II).

6 months after photorefractive keratectomy (PRK) for extreme[5] and moderate myopia.[6] Additionally, it has been suggested that haze may vary not only from one eye to the other in a patient[7,8] but also between different regions in an individual cornea.[8] Therefore, quantification of corneal haze by means of an objective method that cannot only adequately assess the overall amount of opacification, but also analyze its regional variations within the ablation zone, would lead to a better understanding of this phenomenon.

We recently have developed a new technique that enables direct objective measurement of corneal opacification and comparison between different areas at the corneal plane. In this study, we attempted to investigate the relation between the intended correction and the amount of haze after PRK for high myopia by using bidimensional digital image analysis of corneal opacification. Beyond that, we measured regional variations in the distribution of corneal haze in an attempt to find out how homogeneous the total distribution of haze is within the treated area and if changes in the uniformity of haze and in the pattern of its regional distribution over the entrance pupil are associated with increased intended correction and postoperative time after PRK for high myopia.

Patients and Methods

Instrumentation

The components of our system are illustrated in Figure 1. The charge coupled device camera required that the image to be digitized be in the form of a photograph. Anterior segment photographs were obtained using a 75 SL slit-lamp camera (Carl Zeiss, Oberkochen, Germany) that had a light source consisting of an XBO 75 W/2 high-pressure short-arc xenon lamp of the ozone-free type (380053-9870) with an average illuminance of 40.000 sb. Agfachrome 200-asa slide films (Agfa-Gevaert AG, Leverkusen, Germany) were used in every case. A standardized photographic technique with a 1.5-mm–wide, 8-mm–long vertical slit beam and an angle of 45° between the observation and the illumination axis from the temporal side of the eye was used throughout the study. Patients were asked to look at a fixed target to ensure primary position of gaze, and the slit beam was focused on the anterior corneal surface. The instrument's zoom magnification changer was adjusted to a magnification factor of 1. These conditions were found to better highlight the corneal opacification and allow further bidimensional analysis of the treated and untreated areas (Fig 2A). The slide films were developed and the images transformed into glossy color prints (3.9 × 5.9 in).

The color charge coupled device camera (charge coupled device, XC-711P, Sony, Tokyo, Japan) captured the photographs of the corneas under a standardized illumination of 1900 lux.[9] The output of the charge coupled device camera was fed into a PIP-512/1024 video digitizer (Matrox Electronic Systems Limited, Quebec, Canada) installed inside a personal computer (Pentium 90, Intel Corp, Santa Clara, CA), where color images were signal processed and transformed into monochrome pictures.

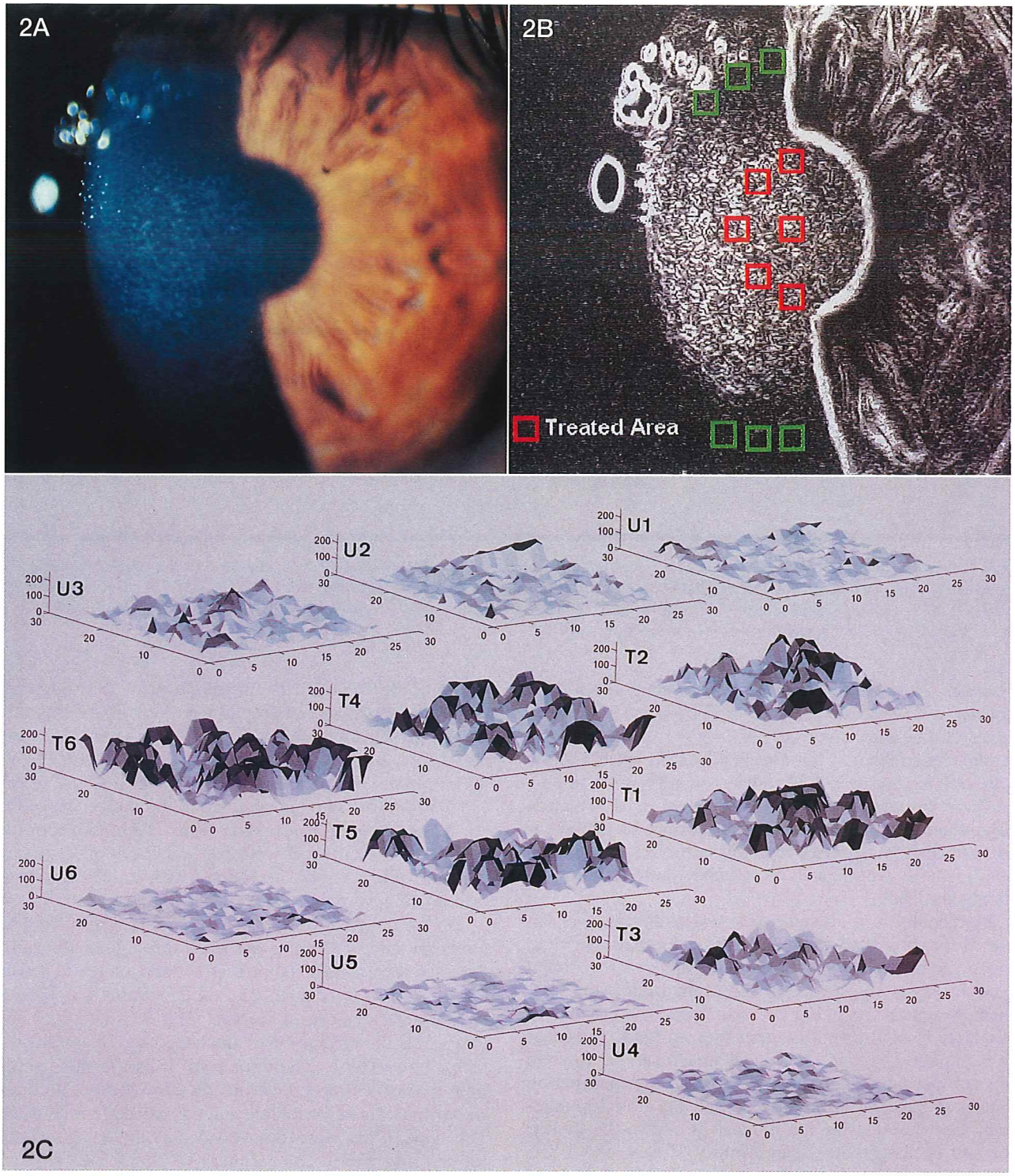

Figure 2. **A,** standardized slit-lamp photograph of a cornea (right eye) that received a −7-diopter correction 4 months ago. This haze was classified as grade 2 (subjective). **B,** the gradient image of the same cornea contains 512 × 512 pixels (horizontal × vertical). Digital image analysis provided an overall quantitative measurement of 48.7 gray levels. **C,** color-coded three-dimensional surface plots correspond to the six regions symmetrically distributed over the entrance pupil (*treated*) and the other six on the adjacent *untreated* cornea that were quantified. In this case, the coefficient of variation of the amount of opacification was 4.3%.

we calculated the mean value of the gray level intensities of the 625 pixels contained within each region delineated on the gradient image. Beyond that, we produced color-coded three-dimensional surface plots using Matlab with Simulink software (version 4.0, The MathWorks, Inc, Natick, MA), which graphically represented the intensity and distribution of gray levels of the gradient image (Fig 2C).

Absolute haze measurements were calculated by subtracting the average of the values obtained for each of the six untreated regions (*U1. . .U6*) from the average of the six treated regions (*T1. . .T6*). Additionally, a clinical grading of anterior stromal haze was carried out independently by an experienced clinical observer (ANT), with the slit-lamp microscope using broad-tangential illumination and the system proposed by Fantes et al.[12] Objective corneal opacity measurements were correlated with subjective assessment of haze, and the association between the attempted correction and the severity of haze, as measured by digital image analysis, also was examined.

To measure variability in the distribution of corneal haze, the differential coefficient of variation (standard deviation/mean) of the values obtained for each of the six treated and the corresponding untreated regions was calculated. This coefficient of variation was correlated with the amount of treatment performed and the postoperative time after PRK. To investigate whether differences between central corneal haze and peripheral haze within the entrance pupil were associated with the attempted correction or the postoperative time, the mean of two subtractions, *T1* minus *T2* and *T1* minus *T3* (Fig 2C), was calculated for each cornea.

Data were plotted on scattergrams, and correlation coefficients were determined for each of the above-mentioned associations. Regression analysis was performed when a straight-line relation between variables was found. Comparison between nominal data was performed using the chi-square test. A two-tailed probability of 0.05 or less was considered statistically significant, and only preplanned comparisons were made to ensure overall protection.

Results

Digital image analysis was performed successfully in each of the 40 eyes presenting variable degrees of corneal haze (Figs 2 and 3). All the cases presented a homogeneous distribution with respect to age and gender, and neither the intended correction nor the administration of steroids nor the time after surgery varied with respect to any of these two variables.

Mean haze values were calculated to be 33.5 plus or minus 20.6 gray levels (range, 3.5–81.5 gray levels). Subjectively, the series presented a wide scope of haze intensity ranging from 0 to 4 (mean ± standard deviation, 1.5 ± 1.1). Mean differences between scarred and clear areas for haze grade 0.5, 1.0, 2.0, 3.0, and 4.0 were 16.9, 26.6, 42.6, 60.4 and 76.4 gray levels, respectively (Fig 4). Direct objective measurements showed excellent correlation with conventional subjective grading ($r_s = 0.96$; $P = 0.0001$).

In our series of patients with high myopia, haze intensity showed a weak direct association with the intended correction ($r = 0.33$). Figure 5 illustrates the relation between the two variables. It was estimated that only 10.8% of the increase in corneal opacity after treatment was because of a greater myopic correction ($R^2 = 0.108$), and this association was statistically significant ($P = 0.037$).

Uniformity in the distribution of haze within the treated area was calculated using the coefficient of variation of the objective measurement values for each eye. Overall, the mean coefficient of variation of the amount of opacification was 9.4 plus or minus 4.7% (range, 2.5%–19.3%). Uniformity in distribution of haze was a feature that showed no significant relation with the intended correction ($r = 0.19$; $P = 0.16$). Mean coefficients of variation in postoperative weeks 4, 8, 12, 18, 24, 32, 40, and 48 were 4.2%, 5.5%, 7.2%, 8.6%, 10.7%, 11.9%, 15.7%, and 16.5%, respectively (Fig 6). Thus, a longer follow-up time associated more heterogeneous haze distribution ($r = 0.88$; $P = 0.0001$). Figures 2 and 3 illustrate respectively the difference between the right and left eyes of the same patient. Although both received a 7-diopter ablation, the right eye, with a 3-month follow-up, showed a more homogeneous distribution of haze (4.5%) than did the fellow eye (10.3%), with a 10-month follow-up. Interestingly, Figure 7 shows that although both ablations were well centered, asymmetry in wound healing on the left eye, as analyzed by videokeratography, closely resembled the subregion over the entrance pupil that showed higher haze measurements (Fig 3).

Overall, the difference in the intensity of corneal haze between the center and more peripheral regions over the entrance pupil for each ablation zone averaged 16.1 plus or minus 13.3 gray levels. This difference was not associated with the amount of treatment performed ($r = 0.23$; $P = 0.45$). However, Figure 8 shows a strong inverse association between greater central corneal haze with respect to the peripheral haze within the entrance pupil and follow-up time ($r = -0.96$; $P = 0.0001$).

Regional variation in corneal topography corresponding to the location of focal haze, as illustrated in Figure 7, was seen in 9 (22.5%) of the 40 eyes. For these nine eyes, the area of haze was the steeper area on the videokeratograph, with mean differences between the steepest and flattest areas in the central 5-mm zone of 2.7 plus or minus 0.8 diopter (range, 0.8–4.0 diopters). The mean postoperative time in this subgroup of eyes was 6.2 months, and none of these correlations between corneal haze and topography were detected before the fourth month. Another striking feature was that this regional variation always occurred for coefficient of variation values over 9% (higher than the mean) and differences in corneal haze intensity between the center and periphery over the entrance pupil of 15 gray levels or less (lower than the average difference of 16.1 gray levels). The shape of the corneal haze in these eyes was arcuate in 5 of them (55.5%), and appeared as an isolated round or oval isle

The image acquisition process was controlled visually on a Trinitron KX-14CP1 television monitor (Sony, Tokyo, Japan) that displayed the picture in gray levels (Fig 1, display I). The video digitizer contained in-house image processing software that enabled not only visualization of the image acquisition process but also recording of the image at 512 × 512-pixel resolutions and 8-bit gray scale for further digital analysis. Both the original and processed digitized images were stored on 3.5-inch floppy disks and either could be displayed on the personal computer monitor (Fig 1, display II, Foxen, Valencia, Spain) or printed out using a Deskjet 850 C color printer (Hewlett-Packard, San Diego, CA).

Image Analysis

The charge coupled device camera was focused on the geometric center of the color photograph of the treated cornea that was presented on the television monitor (Fig 1, display I). The video digitizer converted the signal into a monochrome 512- × 512-pixel image with a resolution of 256 gray levels per pixel. Each of the 262.144 pixels of the image was coded as a bidimensional function of light intensity $f(x, y)$, where f represented the gray level value and x and y were the spatial coordinates of that particular point. In our system, f ranged from 0 to 255, and x and y ranged from 0 to 511 each.

Automated analysis of the images was performed by computing the gradient operator,[10] namely, a derivative operator that detected and enhanced the edge of the discontinuities in the image. The gradient operator highlighted rough areas in the image resulting from intensity differences between adjacent pixels and understated the smooth areas where the differences between adjacent pixels were small. To detect a digital edge, that is to say, the boundary between two pixels that appears when their brightness (gray level intensity) values are significantly different, small spatial masks were used, the centers of which were moved pixel to pixel through the image. These masks consisted of matrixes of three rows and three columns resulting in nine cells that analyzed nine contiguous pixels at once to conform with the edge detector masks described by Prewitt.[11] We used the gradient, a vector $G[f(x, y)]$ that points in the direction of the maximum rate of increase in the function $f(x, y)$ and provides the maximum rate of increase of $f(x, y)$ per unit distance in the direction of $G[f(x, y)]$ to enhance the edge of the discontinuities on the image. We generated gradient images (Fig 2B) based on the use of two masks, one that responded more strongly to edges oriented horizontally and the other that responded more strongly to edges oriented vertically.[10,11] Convolving these masks with an image $f(x, y)$ yielded the gradient at all points in the image resulting in the complete gradient image (Fig 2B). Thus, the magnitude of the gradient was proportional to changes in gray levels and was more prominent in regions of an image containing distinct edges. The average time for this whole analysis was approximately 5 seconds.

Finally, by means of a cursor, six regions in the treated cornea (red squares, *T1. . .T6*) and another six regions in the adjacent untreated cornea (green squares, *U1. . .U6*) were delineated on the gradient image displayed on the personal computer monitor (Fig 2B). Each of these regions was 25- × 25-pixels wide. In the present system, the resolution of 1 pixel corresponds to a distance of 14.3 μm (vertical) and 18.6 μm (horizontal) on the cornea. Therefore, each region contained 625 points and covered an area of the cornea measuring 166,237 μm^2. The location of the six regions delineated within the ablated zone over the entrance pupil is outlined in Figure 2B (red squares). These regions were delineated by the analyzer so as to solely contain distinct edges corresponding to reticular haze, and this process was controlled visually on the monitor (Fig 1, display II). The six regions of the adjacent untreated cornea were delineated, avoiding the intense reflection of the slit beam on the iris anterior surface that was situated nasally. These regions (*green squares*) were used as a control of the measurements made on the treated zone of the same eye and were designed to minimize the bias originated by changes in brightness attributable to proximity to the light source, which was situated temporally (Fig 2A). Care was taken to avoid the *noise* generated in the acquisition process or by the iris crypts.

Patients

The data were collected from 40 PRK procedures in 34 patients at various postoperative intervals (mean ± standard deviation, 21.0 ± 14.5 weeks) with a minimum and a maximum follow-up time of 4 weeks and 1 year, respectively. Measurements were undertaken at a single point in time during the healing period after the excimer laser treatment. All the patients were recruited randomly from an ongoing trial evaluating PRK for high myopia using a MEL-60 eximer laser (Aesculap-Meditec, Heroldsberg, Germany).[5] Informed consent was obtained from all the study participants. The patients in this core trial were on average 31.6 years old (range, 22–52 years), and the proportion of male subjects was 19 (47.5%) of 40. All the subjects had an attempted correction between −6 and −22 diopters (mean, 11.14 diopters), and neither combined astigmatic corrections nor retreatments were included in this series. Details of the ablative procedure and postoperative care have been described elsewhere.[5] Briefly, the excimer laser delivered a fluency of 250 mJ/cm^2 at the cornea with a repetition rate of 20 Hz, using a slit-scan mode of 7 mm × 1 mm to correct high myopia. The optical zone diameter in all eyes was 5 mm, with a 1-mm-wide tapered transition zone.[5] After surgery, fluorometholone 0.25% was administered 5 times a day during the first month and then slowly tapered down over the following 5 months. Wound healing was controlled biomicroscopically, and videokeratography was performed using the Tomey-Computed Anatomy, Topographic Modeling System (Tomey Technology, Inc, Cambridge, MA).

Data Analysis

Using commercially available software (Quattro Pro, version 1.0, Borland International, Inc, Scotts Valley, CA),

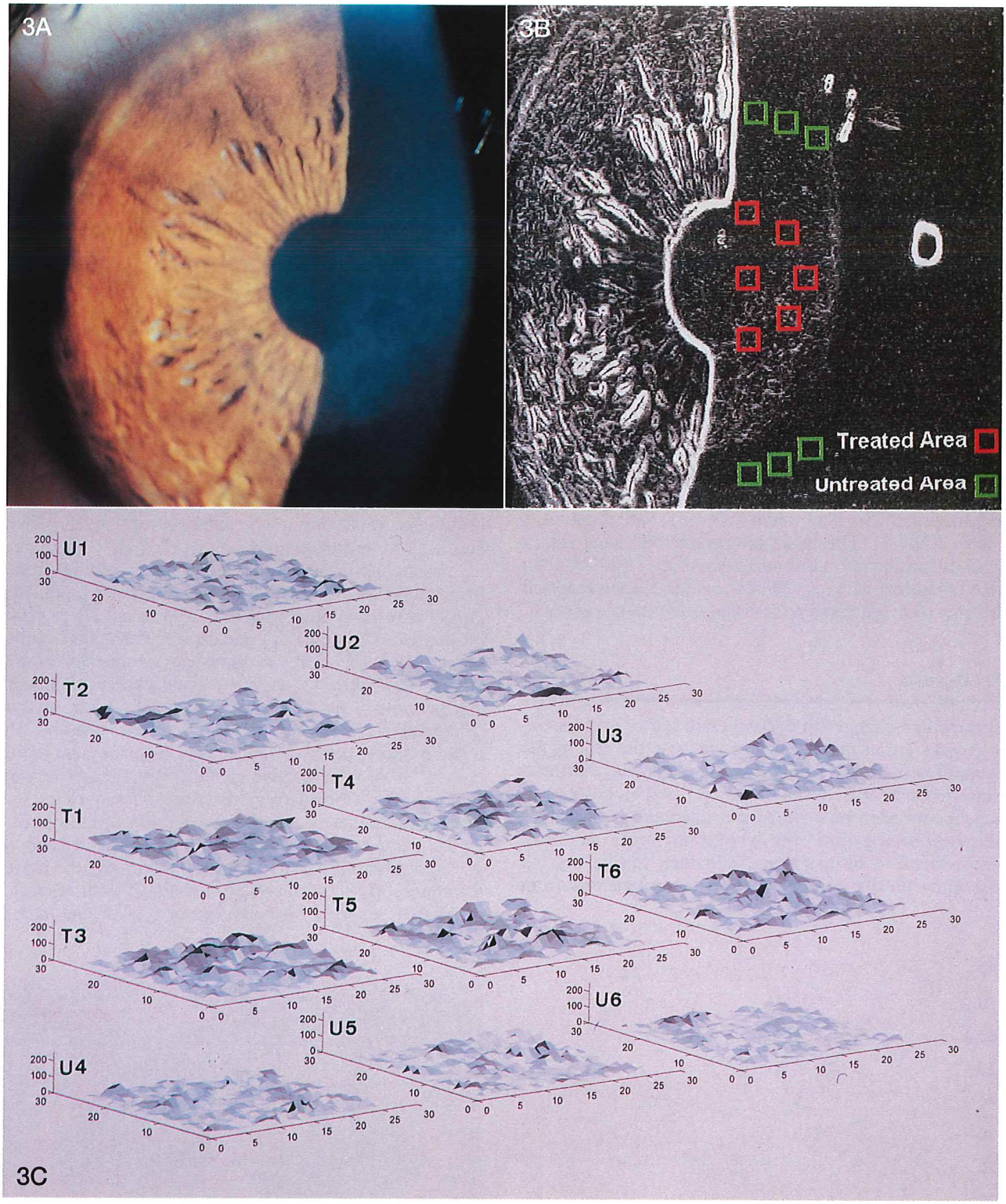

Figure 3. **A,** standardized slit-lamp photograph of the fellow eye (left eye) of the one displayed in Figure 2, which received a −7-diopter correction 10 months ago. This photomicrograph showed inferior arcuate subepithelial haze and was classified as grade 1 (subjective). **B,** the gradient image of the same cornea contains 512 × 512 pixels (horizontal by vertical). Digital image analysis provided an overall quantitative measurement of 19.5 gray levels. **C,** color-coded three-dimensional surface plots correspond to the six regions symmetrically distributed over the entrance pupil (*treated*) and the other six on the adjacent *untreated* cornea that were measured. In this case, the coefficient of variation of the amount of opacification over the entrance pupil was 15.1%.

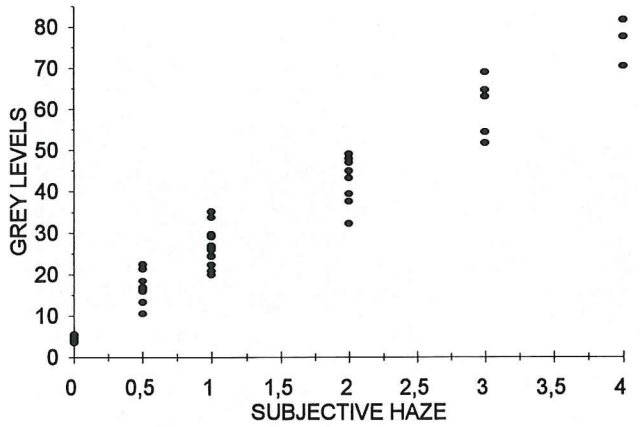

Figure 4. Graph showing the relation between subjective grading of haze and objective quantification by digital image analysis expressed in gray scale levels.

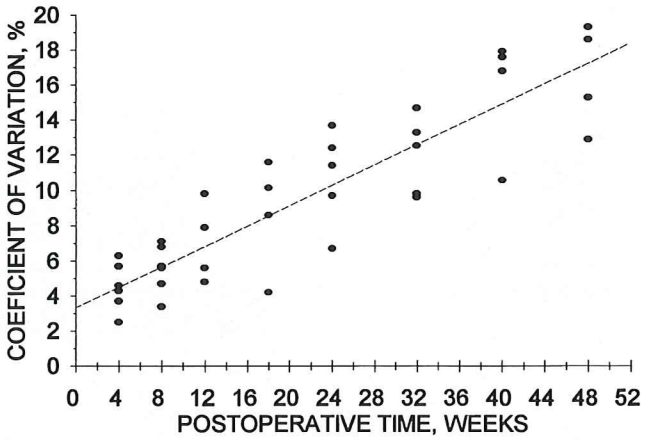

Figure 6. The relation between the coefficient of variation of corneal haze over the entrance pupil, and postoperative time after photorefractive keratectomy for high myopia is direct and linear ($R^2 = 0.78$). The dashed line (y = 3.37 + 0.28 x) was obtained by linear regression for the actual data points (n = 40).

in 4 of them (44.4%). The corresponding topographic patterns were semicircular in 4 of them (44.4%), irregularly irregular[13] in 3 of them (33.3%), and focal in 2 of them (22.2%). The mean best-corrected visual acuity generally was better in this subgroup of eyes (20/25) than in the remaining 31 eyes (20/32), and the 2 main reported problems were glare and poor visual performance at night.

Discussion

Postoperative changes in corneal clarity after excimer laser surgery are of major concern, because the aim of the treatment is to improve uncorrected visual acuity without losing best-corrected visual acuity.[14,15] Although considerable knowledge on laser-tissue interactions and their effects has been gained over the past few years, there still are questions to be answered.[14] In fact, further studies are needed on the possible delayed complications from ultraviolet irradiation of the anterior segment in patients predisposed to greater endothelial cell loss,[16,17] and a better understanding of the corneal wound healing process in response to excimer laser surgery and its modulation also is of primary importance.[6–8] The recent development of improved systems for measuring the actual corneal optical contour[13] and the thickness of anterior corneal layers[18] has helped to identify clinically relevant phenomena previously not fully understood. However, analysis of corneal haze has been as yet limited to methods that make multiple point or serial linear measurements of the cornea[19–24] or to subjective methods that are arbitrary and imprecise.[12,24] Considering the reticular nature of the scarring[25] and the heterogeneous distribution of the opacities across the cornea,[2,4,8] quantification of corneal haze and its regional variations at the corneal plane with the present technique offers an important advantage with respect to previously reported methods. In our system, the average

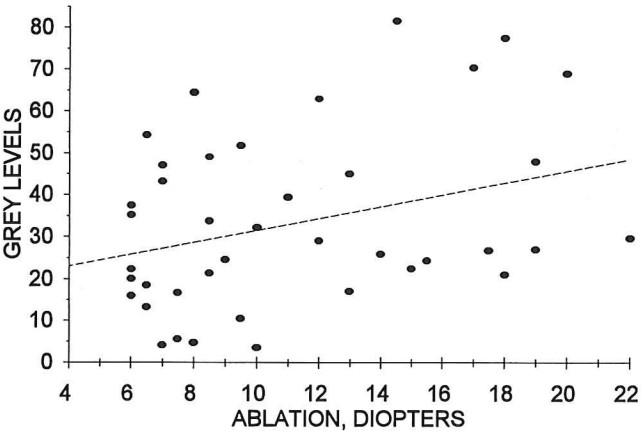

Figure 5. Regression plot of corneal haze intensity versus attempted correction shows a weak association between these two variables ($R^2 = 0.11$). The dashed line (y = 17.4 + 1.46 x) represents the least-square linear fit through the actual data points (n = 40).

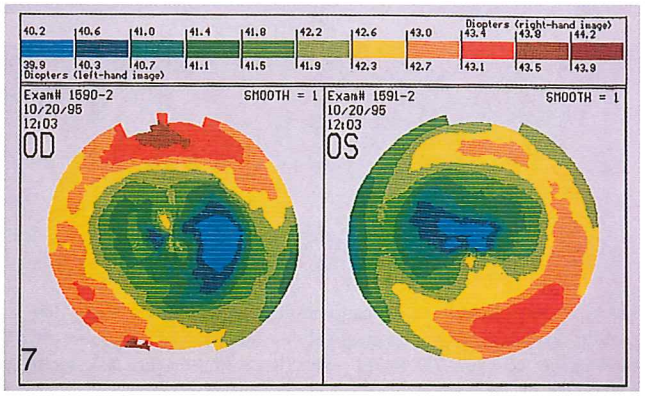

Figure 7. Corneal topographic maps show absence of gross decentration of the ablation zone on the right and left eyes previously shown in Figures 2 and 3, respectively. The steeper zone over the entrance pupil on the left eye corresponds with a subregion with residual haze.

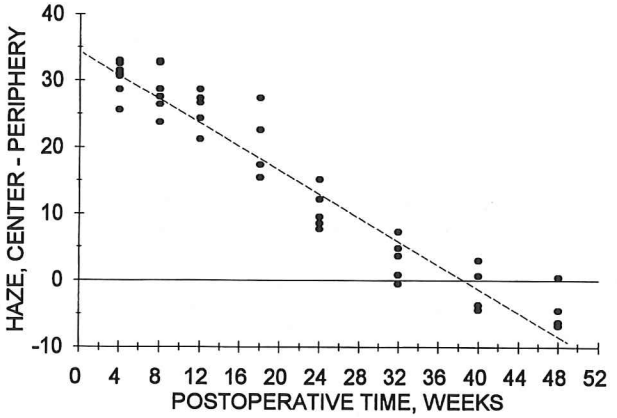

Figure 8. Difference between corneal haze at the center of the cornea and more peripheral opacification expressed in gray scale values versus postoperative time after photorefractive keratectomy for high myopia. A highly significant inverse association was observed ($r = -0.96$; $P = 0.0001$). The dashed line ($y = 34.5 - 0.87\ x$) was obtained by linear regression for the actual data points ($n = 40$).

time for digital image analysis of the anterior segment photographs was approximately 5 seconds. Considering that the spatial resolution of the images resulted in 14.3 × 18.6 μm of the cornea per pixel, our method approached the resolution reported for online Scheimpflug imaging of the cornea.[23]

An important limitation in our system is that corneal haze photographs, which are digitized for further analysis, may be influenced by many variables in the photographic process that can modify the degree of haze. The current image acquisition method could be optimized further by using an integrated vidicon camera as a digitizer, thus avoiding photograph processing. This camera-digitizer device directly would record the natural image of the cornea on the slit lamp and provide a digital output signal.

Direct objective quantification of corneal haze showed excellent correlation with subjective grading performed by an experienced observer, as illustrated in Figure 4. This contrasts with the lack of agreement reported between other objective methods[20,24] and subjective haze scores. Furthermore, whereas ordinal subjective grading scores fall into 6 discrete categories ranging from 0 to 4,[8,12] our technique permits quantification of small increments in opacification and allows classification into a continuous variable that ranges from 3.5 gray levels to 81.5 gray levels (Fig 4).

Previous reports suggest that individual differences in wound healing after photorefractive keratectomy seem to be a more important variable than the ablation depth in the development of haze.[26,27] Using digital image analysis, we found that only 10.8% of the increase in corneal opacity after PRK for high myopia was associated with a greater attempted correction (Fig 5). This finding suggests that for treatments exceeding 6 diopters, haze intensity shows an overall weak direct association with the intended correction ($r = 0.33$; $P = 0.037$).

Our findings also suggest that haze variability can occur in a single cornea and that the heterogenous distribution of haze is associated with longer follow-up (Fig 6). This regional variation has potentially undesirable effects such as focal excess light scattering, causing glare and halos that are more manifest at night. In fact, although intensity seemed a more important factor than uniformity in haze, some of our patients with low haze severity and high coefficient of variation values reported decreased quality of vision. In our study, the excimer laser was calibrated before use to ensure a reasonably uniform beam and consistent pulse energy. All eyes epithelialized within 4 days and showed properly centered ablations on the first videokeratographic examination. A recent case series[8] has shown that variability in wound healing occurs within the ablated area of an individual cornea and can create regional variation in haze and topography without any known causative agent. In this study,[8] authors report that clear areas in the ablation zone correspond to flat zones on the videokeratographs and the areas of subepithelial haze correspond to steeper zones. We have noted such a finding in 9 (22.5%) of the 40 eyes. These eyes presented a remarkable tendency toward high coefficients of variation and reduced differences in corneal haze intensity between the center and periphery over the entrance pupil.

Overall, haze intensity at the center of the ablated area tended to be higher than more peripheral haze over the entrance pupil (mean difference, 16.1 ± 13.3 gray levels). This can be explained by tissue removal from the center being greater than from the midperiphery of the ablated area.[3] However, no significant correlation between the amount of correction and the difference of haze intensity between these two regions could be shown, which suggests that differences in the steepness of the ablation profiles for higher myopias exert no meaningful influence on corneal wound healing at this point. Beyond that, our study found a strong association between diminishing central haze with respect to peripheral regions over the entrance pupil and postoperative time (Fig 8). Examination results with a follow-up exceeding 8 months showed that the haze was relatively less intense at the center of the cornea than in the periphery over the entrance pupil. This may be attributed to abnormal tissue organization being started and resolved first at the site of maximal ablation depth. Regardless of whether this is the cause, the clinical finding may be of relevance when planning excimer laser reoperations for residual haze.

Our study was descriptive of corneal haze and its distribution variation noted at a single point in time during the healing period after PRK for high myopia. Further studies prospectively may analyze changes occurring in a group of eyes over time. Beyond that, the correlation between quantitative values of focal haze by digital image analysis and corneal power on color-coded videokeratographs may be studied extensively. This also would be useful in providing the surgeon with more detailed information for making a decision on focal retreatment for residual haze as an alternative to ablation of the whole zone, similar to what was suggested by Gibralter and Trokel[28] for the correction of irregular astigmatism. In the current study, digital image analysis appeared to be potentially useful as a new technique for quantitatively characterizing corneal

haze. Using digital image analysis, the authors showed that in excimer laser PRK for high myopia, corneal haze uniformity and distribution pattern appear to be time-dependent parameters. Beyond that, the associations herein described may provide useful information for a better understanding and management of corneal haze after PRK.

References

1. Seiler T, Holschbach A, Derse M, et al. Complications of myopic photorefractive keratectomy with the excimer laser. Ophthalmology 1994;101:153–60.
2. Gartry DS, Kerr Muir MG, Marshall J. Photorefractive keratectomy with an argon fluoride excimer laser: a clinical study. Refract Corneal Surg 1991;7:420–35.
3. McDonald MB, Liu J, Byrd RJ, et al. Central photorefractive keratectomy for myopia: partially sighted and normally sighted eyes. Ophthalmology 1991;98:1327–37.
4. Seiler T, Kahle G, Kriegerowski M. Excimer laser (193 nm) myopic keratomileusis in sighted and blind human eyes. Refract Corneal Surg 1990;6:165–9.
5. Menezo JL, Martinez-Costa R, Navea A, et al. Excimer laser photorefractive keratectomy in high myopia. J Cataract Refract Surg 1995;21:393–7.
6. Carr JD, Patel R, Hersh PS. Management of late corneal haze following photorefractive keratectomy. J Refract Surg 1995;11(Suppl):S309–13.
7. Gartry D, Kerr Muir M, Lohmann C, Marshall J. The effect of topical corticosteroids on refractive outcome and corneal haze after photorefractive keratectomy: a prospective, randomized, double-blind trial. Arch Ophthalmol 1992;110:944–52.
8. Grimm B, Waring GO III, Ibrahim O. Regional variation in corneal topography and wound healing following photorefractive keratectomy. J Refract Surg 1995;11:348–57.
9. Artigas JM, Capilla P, Felipe A, Pujol L. Optica fisiológica. Psicofísica de la visión. 1st ed. Madrid: McGraw-Hill, 1995;41–70.
10. Gonzalez RC, Wintz P. Digital image processing. 2nd ed. vol. I. Reading: Addison-Wesley Publishing Company, 1987;331–50.
11. Haralick RM, Shapiro LG. Computer and robot vision. 2nd ed. vol. I. Reading: Addison-Wesley Publishing Company, 1992;337–46.
12. Fantes FE, Hanna KD, Waring GO III, et al. Wound healing after excimer laser keratomileusis (photorefractive keratectomy) in monkeys. Arch Ophthalmol 1990;108:665–75.
13. Hersh PS, Schwartz-Goldstein BH. Corneal topography of Phase III excimer laser photorefractive keratectomy: characterization and clinical effects. Ophthalmology 1995;102:963–78.
14. McDonnell PJ. Excimer laser photorefractive keratectomy: the Food and Drug Administration Panel speaks [editorial]. Arch Ophthalmol 1995;113:858–9.
15. Steinert RF. Therapeutic keratectomy: corneal smoothing. In: Thompson FB, McDonnell PJ, eds. Excimer Laser Surgery: The Cornea. 1st ed. New York: Igaku-Shoin, 1993; chap. 9:121–9.
16. Maldonado MJ, Menezo JL. The corneal endothelium and myopic excimer laser photorefractive keratectomy [letter]. Arch Ophthalmol 1995;113:697.
17. Maldonado MJ, Navea-Tejerina A, Menezo JL. Human corneal endothelium after excimer laser PRK [letter]. Ophthalmology 1995;102:1736–7.
18. Reinstein DZ, Silverman RH, Trokel SL, Coleman J. Corneal pachymetric topography. Ophthalmology 1994;101:432–8.
19. Andrade HA, McDonald MB, Liu JC, et al. Evaluation of an opacity lensometer for determining corneal clarity following excimer laser photoablation. Refract Corneal Surg 1990;6:346–51.
20. Lohmann CP, Gartry D, Kerr Muir M, et al. Corneal haze after excimer laser refractive surgery: objective measurements and functional results. Eur J Ophthalmol 1991;1:173–80.
21. Lohmann CP, Timberlake GT, Fitzke FW, et al. Corneal light scattering after excimer laser photorefractive keratectomy: the objective measurements of haze. Refract Corneal Surg 1992;8:114–21.
22. Allemann N, Chamon W, Silverman RH, et al. High-frequency ultrasound quantitative analyses of corneal scarring following excimer laser keratotomy. Arch Ophthalmol 1993;111:968–73.
23. Huebscher HJ, Schmidt H. On-line Scheimpflug imaging and its potential for in vivo examination of cornea and lens. Ophthalmic Res 1994;26(Suppl):33–8.
24. Cherny M, Stasiuk R, Kelly P, et al. Computerised Scheimpflug densitometry as a measure of corneal opacification following excimer laser surgery. Ophthalmic Res 1994;26(Suppl):48–54.
25. Lohmann CP, Gartry D, Kerr Muir M, et al. Haze in photorefractive keratectomy: its origins and consequences. Lasers and Light in Ophthalmology 1991;4:15–34.
26. Sher NA, Barak M, Daya S, et al. Excimer laser photorefractive keratectomy in high myopia. Arch Ophthalmol 1992;110:935–43.
27. Seiler T, Derse M, Pham T. Repeated excimer laser treatment after photorefractive keratectomy. Arch Ophthalmol 1992;110:1230–3.
28. Gibralter R, Trokel SL. Correction of irregular astigmatism with the excimer laser. Ophthalmology 1994;101:1310–5.